Enhanced Thermal Stability of W-Ni-Al[subscript 2]O[subscript 3] Cermet-Based Spectrally Selective Solar Absorbers with W Infrared Reflectors

Enhanced Thermal Stability of W-Ni-Al_2O_3 Cermet-based Spectrally Selective Solar Absorbers with W Infrared Reflector

Feng Cao, Daniel Kraemer, Tianyi Sun, Yucheng Lan, Gang Chen, and Zhifeng Ren**

Dr. F. Cao,[+] Dr. T. Y. Sun, Dr. Y. C. Lan, and Prof. Z. F. Ren

Department of Physics and TcSUH, University of Houston, Houston, Texas 77204, USA

Email: zren@uh.edu

Mr. D. Kraemer,[+] and Prof. G. Chen

Department of Mechanical Engineering, Massachusetts Institute of Technology, Cambridge, Massachusetts 02139, USA

Email: gchen2@mit.edu

Dr. T. Y. Sun

Department of Physics, Boston College, Chestnut Hill, Massachusetts 02467, USA

[+] F. C. and D. K. contributed equally to this work.

Keywords: solar absorber, cermet, solar absorptance, thermal emittance, spectral selectivity

Solar thermal technologies such as solar hot water and concentrated solar power trough systems rely on spectrally-selective solar absorbers. These solar absorbers are designed to efficiently absorb the sunlight while suppressing re-emission of infrared radiation at elevated temperatures. Efforts for the development of such solar absorbers must not only be devoted to their spectral selectivity but also to their thermal stability for high temperature applications. In this work selective solar absorbers based on two cermet layers are fabricated using a magnetron sputtering technique on mechanically

polished stainless steel substrates. The targeted operating temperature is 500 – 600 ℃. However, we observed a detrimental change in the morphology, phase, and optical properties if the cermet layers are deposited on a stainless steel substrate with a thin nickel adhesion layer, which is due to the diffusion of iron atoms from the stainless steel into the cermet layer forming a $FeWO_4$ phase. In order to improve thermal stability and reduce the infrared emittance, we find tungsten to be a good candidate for the infrared reflector layer due to its excellent thermal stability and low infrared emittance. We demonstrate a stable solar absorptance of ~0.90 and total hemispherical emittance of 0.15 at 500 ℃.

1. Introduction

Since ancient times mankind has converted sunlight into a useful terrestrial heat source by means of sunlight absorbing surfaces. Nowadays, solar absorbers find applications in well-established solar thermal systems such as solar hot water systems and concentrated solar power (CSP) trough systems, also in emerging technologies such as solar thermoelectric, solar thermophotovoltaic, and solar thermionic generators.[1] The solar thermal receiver efficiency is strongly dependent on the optical properties of the solar absorber. To maximize efficiency solar absorbers should exhibit a near-blackbody absorptance (α) in the solar spectrum range while retaining a low emittance (ε) in the infrared (IR) range,[2, 3] and be thermally stable at their operational temperatures.

As for mid-temperature (100 ^{o}C < T < 400 ^{o}C) and high-temperature (T > 400 ^{o}C), cermet-based coatings made of ceramic metallic composites are considered to be good candidates due to their high solar absorptance, low emittance and good thermal stability because of the high temperature stable ceramic host.[2, 4] Cermet-based spectrally selective solar absorbers have been developed and studied as single, double, and triple cermet layers. The thin cermet layer is typically

deposited onto a metallic surface for high solar absorptance while being transparent to IR radiation. The absorption of solar radiation in the cermet layer is mostly caused by interband transitions in the metal and small particle plasmonic resonances. A graded metal volume fraction within the cermet layer gives it a gradual increase in the refractive index from surface to the substrate which reduces reflection compared with single cermet layer absorbers that often use black metals such as black chrome, black nickel, or black tungsten as their metal fillers. Similar to a graded cermet, cermet multilayers with different metal volume fractions introduce a stepwise change in the refractive index resulting in a low reflection of visible light due to interference effects. Additional antireflection coatings are typically applied to further reduce reflection losses. Consequently, cermet-based solar absorbers have a large tunable parameter space from constituents, coating thicknesses to particle concentration, size, shape and orientation to optimize their spectral selectivity. Thus, a lot of cermet-based solar absorbers have been studied to date. Various combinations of host materials such as Al_2O_3, AlN, and SiO_2 with metallic filler atoms such as Ni, Co, Ti, Mo, W, Pt, SS, Cu, Ag, Au have been investigated in terms of the optical performance and thermal stability of the cermet surfaces.[5, 6, 7-9] They all have ceramic host materials in common that naturally possess high temperature stability. The metal filler atoms must be chosen for their high melting point and their nitriding and oxidation resistance to ensure thermal stability. In the case of solar absorbers with mid-temperature applications, the cermet layers are deposited on metal substrates such as polished aluminum or copper due to their low IR emittance and high thermal conductivity. For example solar absorbers based on an Al_2O_3 host material have shown excellent optical properties.[5, 7, 10] However, there are only few reports regarding the investigation of high temperature stability in particular long term thermal stability at 600 ℃ or higher. For example, Mo-Al_2O_3 cermet coatings deposited on stainless steel (SS) are proven to be stable at 800 ℃ for 2 hrs in

vacuum.[9] Antonaia *et al.* replaced Mo with W and found a slight change in the reflection spectra after annealing at 580 ^{o}C for 2 days in vacuum.[8] Mo-SiO_2 cermet based solar spectrally selective absorbers deposited on SS also displayed a high solar absorptance of 0.94 and a very low thermal emittance at 580 ^{o}C.[11] Bare copper and aluminum are excluded as substrate material for high temperature solar absorbers due to the low melting point of aluminum and the high elemental diffusion of copper atoms at high temperature. Optically thick metal layers such as Mo, W, or Ni deposited on non-metallic substrates (quartz, silicon) or on high-temperature stable alloys are possible alternatives. Stainless steel was also studied as a potential candidate as substrate for high-temperature solar absorbers due to its thermal stability, however, the diffusion of iron and carbon atoms into the cermet layers at high temperature alter the optical properties over time. As a solution a diffusion barrier between the substrate and the cermet layer was introduced with a spontaneously formed Fe_2O_3 layer by annealing the stainless steel substrate at 500 ℃ in air.[7] However the roughness of the substrate changes a lot when forming a Fe_2O_3 layer, which eventually affects the roughness of solar absorber and then increases the emittance. Also, the Fe_2O_3 layer on the backside of the stainless steel also introduces another thermal resistance layer in solar absorber, which will decrease the heat transport efficiency from the absorber to the thermal system.

Our strategy is to deposit a nickel (Ni) or tungsten (W) layer onto the mechanically polished stainless steel substrate to act as a diffusion barrier and as a low IR emittance coating to improve spectral selectivity. We investigate the performance of the metal IR reflector layer with a double-layer cermet structure and two antireflection coatings (ARCs). In contrast to typical cermet structures that are filled with particles of one metal type, our cermet layers based on an Al_2O_3 ceramic host material are filled with high temperature stable Ni-W alloy prepared by co-sputtering. This has the advantage that not only the metal volume fraction in each cermet layer but also the

volume fraction of the individual constituent can be adjusted to tailor the optical properties. The individual layers of the solar absorbers are deposited with a magnetron sputtering technique. The spectral bidirectional reflectance responses of the fabricated solar absorbers are measured at room temperature before and after annealing at 600 ℃ for 7 days. The solar absorptance and total hemispherical emittance are also measured at elevated temperatures of up to 500 ^{o}C.

2. Results and discussion

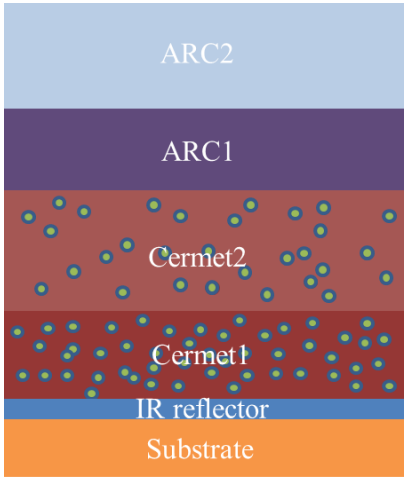

Figure 1. Schematic of wavelength selective solar absorber structure with a double antireflection coating (ARC1 and ARC2), a double cermet layer (Cermet1 and Cermet2), and a metallic IR reflector layer (IR reflector) deposited onto a metal (stainless steel) substrate.

The fabricated and tested spectrally selective solar absorbers for mid- and high-temperature applications are based on a double cermet layer configuration with two ARC layers and a metal layer with high IR reflectance as diffusion barrier (**Figure 1**). The two ARC layers ARC1 and ARC2 are Al_2O_3 and SiO_2 thin films, respectively. In order to investigate the effect of the IR reflector layer the solar absorber multilayer structures are fabricated with tungsten, optically thick nickel, or very thin nickel layer as IR reflector or bonding layer. The detailed parameters are summarized in **Table 1**.

Table 1. Sputtering parameters of optimized solar selective absorbers

Metal layer: a DC power density of 12.3 W/cm^2 for nickel, and a DC power density of 2.2 W/cm^2 for tungsten.

Cermet1: W+Ni+Al_2O_3 with a DC power density of 0.33 W/cm^2 for tungsten and 0.99 W/cm^2 for nickel, and a RF power density of 9.9 W/cm^2 for Al_2O_3.

Cermet2: W+Ni+Al_2O_3 with a DC power density of 0.26 W/cm^2 for tungsten, and 0.74 W/cm^2 for nickel, and a RF power density of 9.9 W/cm^2 for Al_2O_3.

ARC1: Al_2O_3 with a RF power density of 9.9 W/cm^2.

ARC2: SiO_2 with a RF power density of 4.4 W/cm^2.

Sample	Substrate	Bonding layer/IR layer	Cermet1	Cermet2	ARC1	ARC2
C1	SS	10 nm Ni	180 nm	NA	NA	NA
C2	SS	10 nm Ni	NA	140 nm	NA	NA
S-SS	SS	10 nm Ni	11 nm	28 nm	25 nm	55 nm
S-Ni/SS	SS	300 nm Ni	11 nm	28 nm	25 nm	55 nm
S-W/SS	SS	300 nm W	11 nm	28 nm	25 nm	55 nm
S-W/SS-2	SS	200 nm W	11 nm	28 nm	25 nm	55 nm
S-W/SS-3	SS	100 nm W	11 nm	28 nm	25 nm	55 nm
S-W/SS-4	SS	50 nm W	11 nm	28 nm	25 nm	55 nm
S-W/SS-5	SS	10 nm W	11 nm	28 nm	25 nm	55 nm

The multilayer stack of our fabricated spectrally selective solar absorbers comprises one bonding or IR reflector layer, double cermet absorption layers and double ARC layers which further reduce reflection in the visible range.[12] The use of mechanically polished stainless steel as the substrate has the advantage of good high temperature stability and low cost, which can promote large scale deployment as a potential solar absorber candidate in high temperature solar receivers. It has been shown that elemental diffusion of iron and carbon from a stainless steel into the cermet layer can be detrimental for the optical properties, which requires a diffusion barrier.[7] Thus, we investigate the thermal stability of our optimized coatings on stainless steel with a 10 nm thin nickel bonding layer (S-SS). Details about multilayer stack composition and preparation parameters are summarized in **Table 1**. The bidirectional reflectance spectra of the pristine and annealed solar absorber are displayed in **Figure 2**. The reflectance of the pristine sample is close to zero in the visible range, which is expected for a double-cermet-absorption-layer combined with a double-ARC-layer due to the intrinsic absorption of the double-cermet layer and the reflectance reducing interference effects.[13] The sharp transition wavelength range from low reflectance to high reflectance appears to be from ~1 to ~3 μm, which can result in promising spectral selectivity even at high temperatures. However, the degraded optical properties of the solar absorber upon annealing at 600 ℃ for 7 days show a detrimental effect on spectral selectivity. The spectral reflectance below ~1.1 μm increases while it decreases above ~1.1 μm which results in a broadening of the transition wavelength range and ultimately decreases the solar absorptance and increases the IR emittance.

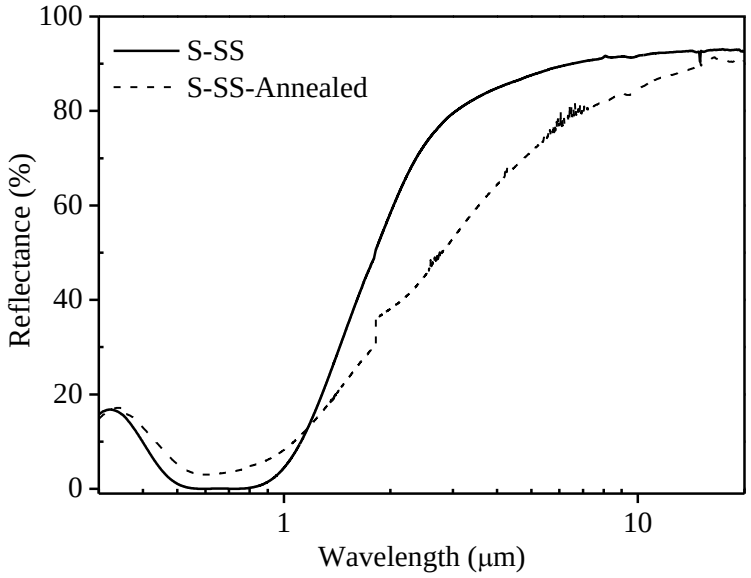

Figure 2. Spectral bidirectional reflectance of a solar absorber with double antireflection coating, double cermet layer, and 10 nm thin nickel layer deposited on a mechanically polished stainless steel substrate before (solid line) and after annealing at 600 ℃ (dashed line).

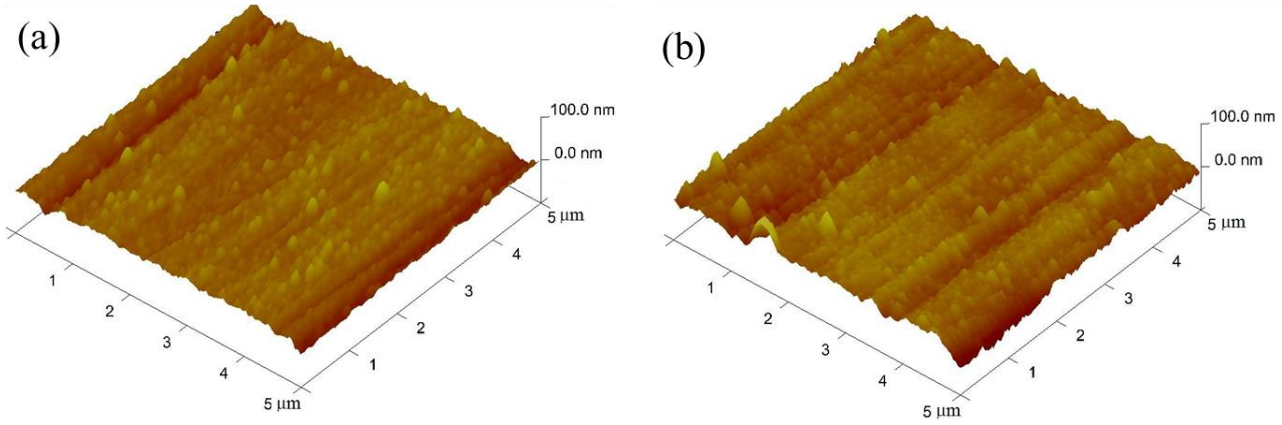

Figure 3. AFM images of S-SS solar absorber with 10 nm thin nickel layer before (a) and after annealing at 600 ℃ for 7 days (b).

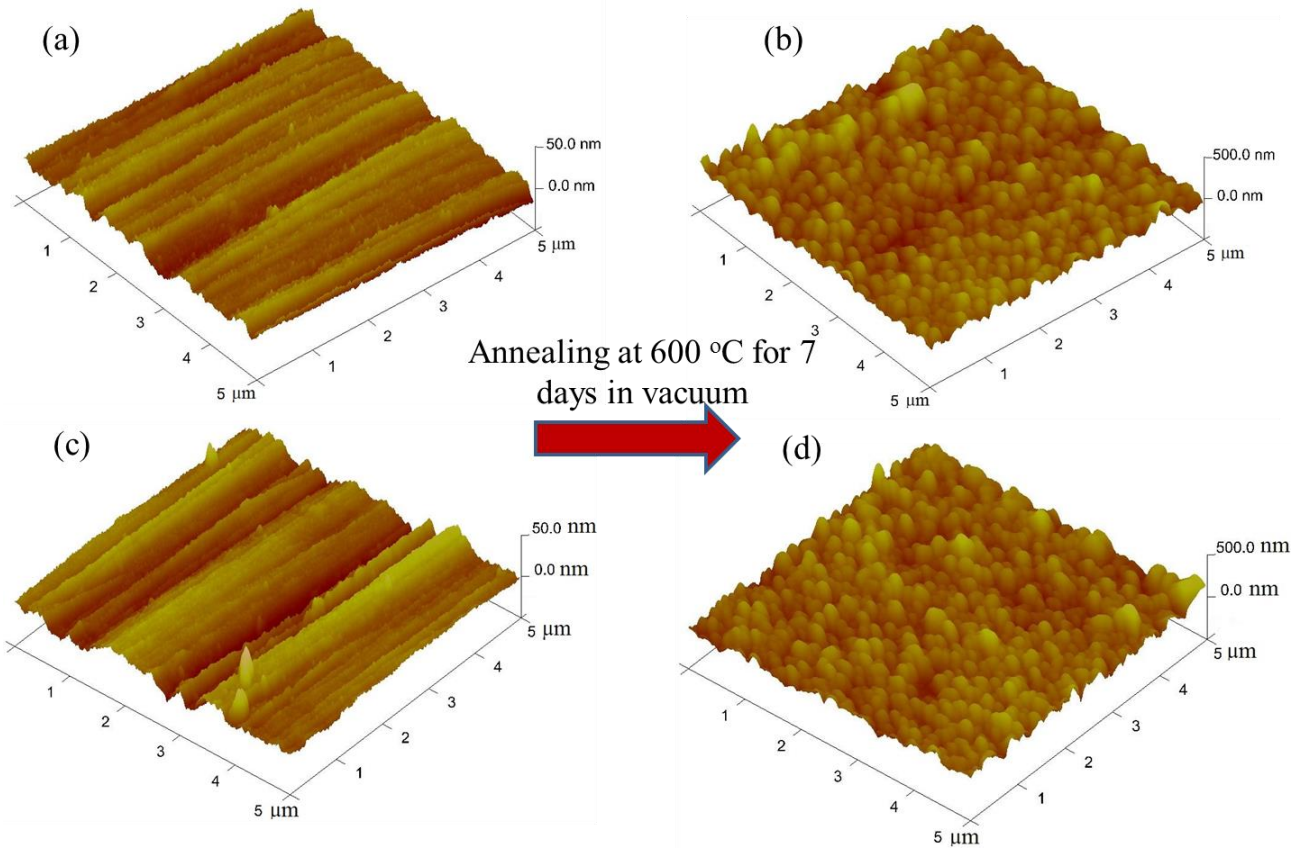

Figure 4. AFM images showing the morphology change of single cermet layer deposited on mechanically polished stainless steel substrate coated with 10 nm Ni layer without any ARC layer upon annealing at 600 °C for 7 days. Cermet1 (C1) with high metal volume fraction in Al_2O_3 host before annealing (a) and after annealing (b), cermet2 (C2) with low metal volume fraction in Al_2O_3 host before annealing (c) and after annealing (d).

A change in the surface roughness of the absorber upon annealing as the cause for the change in optical properties can be excluded (**Figure 3**). No significant surface roughness change upon sample annealing is observed. The sample retains the groove structure created by the mechanical polishing process applied to the stainless steel substrate. The root mean square roughness (Rq) of the sample before and after annealing is calculated to be $6-8$ nm using a NanoScope Analysis software.

To further explore possible causes for the change in optical properties at high temperatures, we investigate two additional cermet samples, C1 and C2, without ARC layers in terms of their phases and morphology before and after annealing (**Figure 4**). The multilayer stacks deposited onto the stainless steel substrates consist of a 10 nm nickel bonding layer and a single cermet layer with the only difference between the two samples being the metal particle concentration in the cermet layers and their thicknesses (C1 and C2, detailed in **Table 1**). Both samples show significant changes in their film morphology upon annealing. Similar to the previous sample (S-SS), the C1 and C2 samples start out with a groove surface structure, however, the annealing process leads to a rapid growth of the Ni-W alloy within the cermet layer from diameters of ~80 nm to 300 – 400 nm. And the roughness increases from 6 – 8 nm to 47-50 nm. The difference in the metal volume fraction and layer thickness between sample C1 and C2 does not affect the particle growth and roughness change. However, the unchanged roughness of the previous sample (S-SS) with double ARC and much thinner double-cermet layer suggests that the ARC layers suppress the particle growth within the cermet or the particle growth is much less pronounced in significantly thinner cermet layers. A phase analysis before and after annealing is conducted using X-ray diffraction and show the sharp peaks for the stainless steel substrate and the Ni-W alloy in the single-cermet layers (**Figure 5**). As expected no diffraction peaks are observed for the dielectric Al_2O_3 even after annealing at 600 ℃ for 7 days due to its stable amorphous nature. However, X-ray diffraction spectra show an additional monoclinic $FeWO_4$ phase after sample annealing. As reported in literature iron atoms diffuse at high temperatures from the stainless steel substrate into the cermet layer.[7] Those iron atoms react with tungsten and residual oxygen to form the observed $FeWO_4$ phase. This result is further supported by Raman measurements showing two distinct peaks located at 882 cm^{-1} and 691 cm^{-1} for the annealed samples which can be traced back to A_g modes of $FeWO_4$

(**Figure 6**).[14] Although we cannot detect the $FeWO_4$ phase in the solar absorber with thin Ni layer (S-SS) due to the small thickness of cermet which significantly limits the signal strength in our equipment, there is no apparent reason why the formation of this phase from Fe, W, and residual oxygen should be suppressed by the anti-reflection coating. Also, the solar absorber with thin nickel layer (S-SS) after annealing displays a very low reflectance in mid-IR range compared to that before annealing (**Figure 2**), indicating a destruction of IR reflector and a formation of nonmetallic phase between substrate and coatings. Thus, the main cause for the degradation of the optical properties for our solar absorber sample (S-SS) probably is the formation of $FeWO_4$ phase in the cermet layers at high temperature.

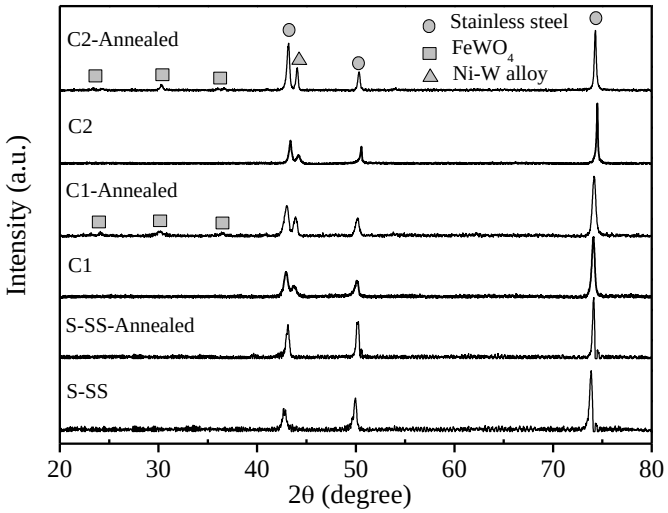

Figure 5. XRD patterns of pristine and annealed cermet coatings with 10 nm nickel layer on stainless steel (C1 and C2) and the solar absorber with thin nickel layer (S-SS). The results show peaks for the stainless steel substrate (solid circles), the Ni-W alloy in cermet,[15] (solid triangles) and the $FeWO_4$ phase (solid squares) for the annealed samples.

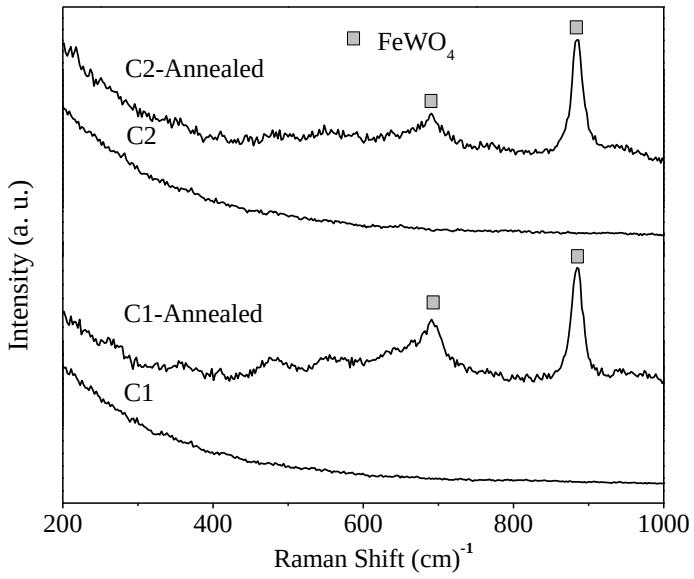

Figure 6. Raman spectra of pristine and annealed cermet coatings with 10 nm nickel on stainless steel substrate (C1 and C2). Two distinct peaks are observed (solid squares) for the $FeWO_4$ phase.

With this result in mind we fabricated solar absorber samples (S-Ni/SS and S-W/SS, **Table 1**) with 300 nm thick metal layers as the diffusion barrier between the stainless steel substrate and the double cermet layer. Nickel and tungsten are chosen as the metal due to their high melting point and low IR emittance which improves the spectral selectivity of the solar absorber compared to the previous sample S-SS with a very thin nickel layer (**Figure 7**). Both thick metal layers significantly increase the spectral reflectance in the mid-IR range without altering the spectral response below 2.5 μm, however only the tungsten layer shows promising high temperature thermal stability. XRD measurements support this result (**Figure 8**). The sample with the thick nickel layer (S-Ni/SS) shows two nickel peaks which disappear after sample annealing suggesting that the nickel reacts with iron atoms from the SS substrate. This is not the case for the sample with a thick tungsten layer (S-W/SS) which is not affected by the sample annealing, thus, demonstrating a stable tungsten layer which prevents the iron diffusion.

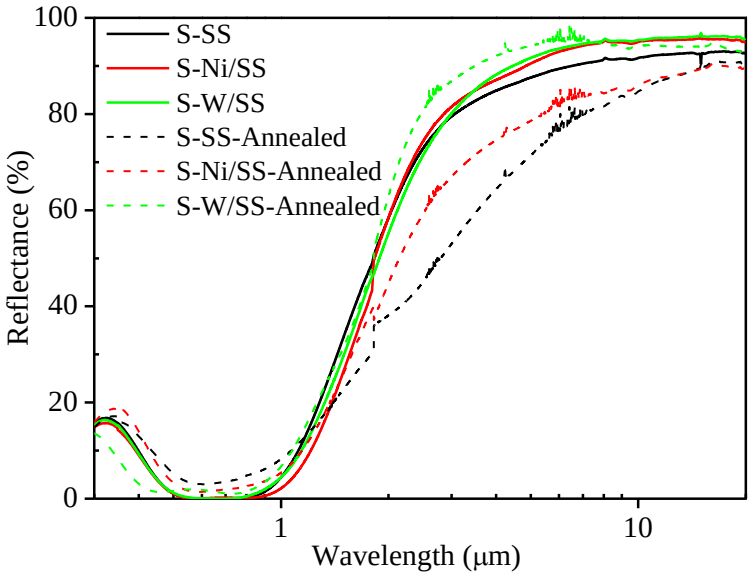

Figure 7. Spectral bidirectional reflectance response of solar absorbers with 300 nm thick tungsten (green line) or nickel IR reflector layer (red line) before (solid lines) and after annealing at 600 ℃ for 7 days (dashed lines). For comparison, the data of the solar absorber sample with a 10 nm thin nickel layer (S-SS, black line) are included.

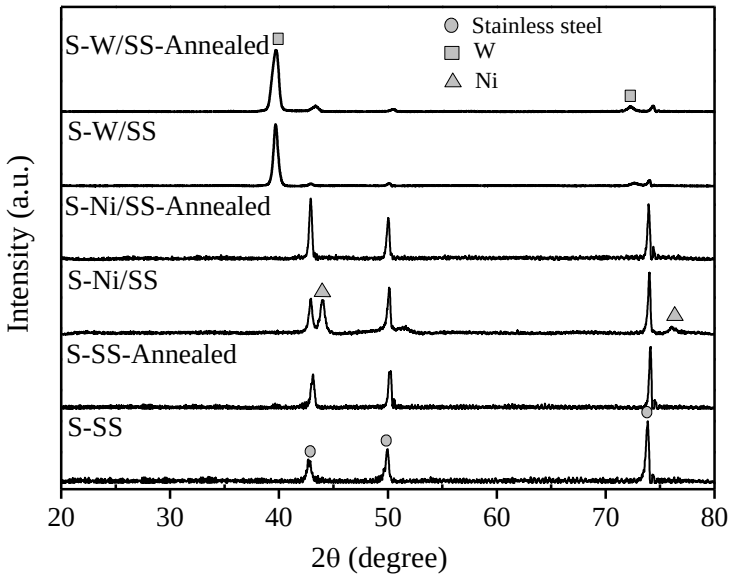

Figure 8. XRD patterns of solar absorbers with different IR reflectors before and after annealing. The peaks marked with solid circles, solid triangles and solid squares come from the stainless steel substrate, nickel, and tungsten layer, respectively.

Table 2. Calculated solar absorptance based on AM 1.5 direct + circumsolar solar spectrum and total bidirectional emittance (82 ℃) of fabricated solar absorbers. S-SS is the absorber with thin 10 nm nickel bonding layer; S-Ni/SS is the absorber with 300 nm nickel IR reflector and S-W/SS is the absorber with 300 nm tungsten IR reflector.

Sample	**Before Annealing**		**After Annealing**	
	Absorptance	**Emittance**	**Absorptance**	**Emittance**
S-SS	91.70%	8.63%	90.66%	15.99%
S-Ni/SS	93.10%	5.46%	91.38%	14.10%
S-W/SS	92.20%	5.65%	90.77%	5.70%

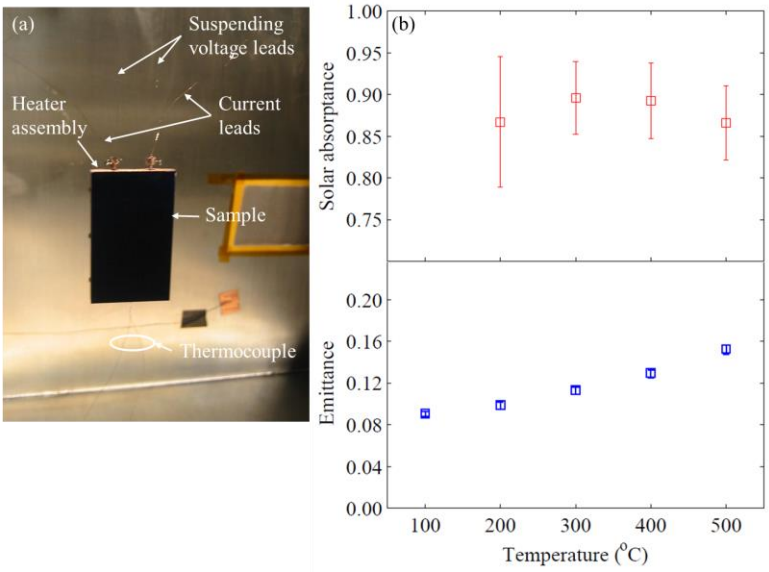

Figure 9. Absolute and direct steady state calorimetric measurements. (a) Experimental setup. (b) The near normal solar absorptance and total hemispherical emittance of a solar absorber with 300 nm tungsten IR reflector (S-W/SS) as a function of temperature.

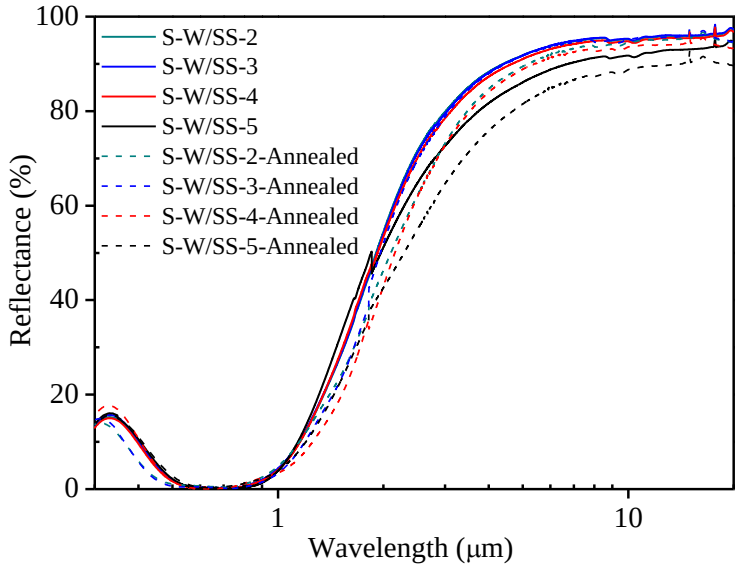

Figure 10. Spectral bidirectional reflectance of solar absorbers with different thicknesses of tungsten IR reflector before (solid lines) and after annealing at 600 ℃ for 7 days (dashed lines). S-W/SS-2, S-W/SS-3, S-

W/SS-4, and S-W/SS-5 are the solar absorbers with tungsten IR reflector of 200 nm (green line), 100 nm (blue line), 50 nm (red line), and 10 nm (black line), respectively.

The near normal solar absorptance and total bidirectional emittance are calculated from the spectral reflectance data suggesting our developed spectrally selective solar absorber with tungsten infrared reflector layer can be a good candidate for high temperature solar thermal applications (**Table 2**). As described in section 2 the spectral properties are obtained at near room temperature and at only one angle, thus, calculating the solar absorptance and total hemispherical emittance for high temperatures using the spectral data can only be used as a rough estimate. From experience the total hemispherical emittance values in particular are significantly underestimated.[2, 16] In order to obtain an accurate estimate of the optical properties at elevated temperature we measured the solar absorptance and the total hemispherical emittance of a sample with a tungsten infrared reflector (S-W/SS) at elevated temperatures up to 500 ℃ (**Figure 9**). The near normal solar absorptance (divergence half angle of ~15 °) is close to independent of temperature with a value of ~0.9 which is in good agreement with the calculated solar absorptance from the spectral data. It has been theoretically shown that cermet-based solar absorbers exhibit a solar absorptance with only weak angle dependence.[17] Thus, only little deviation from here demonstrated solar absorptance should be expected even for concentrated solar power applications with a large range of incident angles. However, future research efforts could experimentally investigate the angle dependence of the solar absorptance to quantify the effect. The total hemispherical emittance shows the typical temperature dependence of a spectrally selective solar absorber with approximately 0.09 at 100 ℃ and 0.15 at 500 ℃.

The tungsten metal layer thickness should be optimized to keep the production cost minimal without losing the low emittance and long term thermal stability of the solar absorber. For that

matter we fabricated several solar absorbers with tungsten layer thicknesses of 10, 50, 100, and 200 nm (**Table 1**) and compare their spectral properties before and after the annealing at 600 ℃ for 7 days (**Figure 10**). For the pristine samples the tungsten layer thickness only affects the spectral reflectance at wavelength larger ~2 μm. The annealing process, however, alters the spectral response in the complete wavelength range with the largest effect at wavelengths longer than ~1.2 μm. As expected the spectral reflectance increases and the thermal stability improves with increasing tungsten layer thickness. A tungsten layer thickness of 100 nm is sufficient to provide good thermal stability and to act as a low emittance coating on stainless steel at high temperatures.

3. Conclusions

We developed a spectrally selective solar absorber based on double cermet layers (W-Ni-Al_2O_3 cermet) with double antireflection layers on a mechanically polished stainless substrate. Iron atoms diffusing from the stainless steel substrate into the cermet layer detrimentally affect the optical properties. A 100 nm thick tungsten layer can suppress the degradation of the optical properties at high temperatures and lowers the emittance relative to the stainless steel substrate, which improves the spectral selectivity of the solar absorber, and Ni is not effective as Fe diffusion barrier and IR reflector. We experimentally demonstrated a solar absorber with a solar absorptance of ~0.9 and total hemispherical emittance of ~0.15 at an operating temperature of 500 ℃.

4. Experimental Section

The spectrally-selective solar absorbers are deposited onto a mechanically polished stainless steel substrate using a commercial magnetron sputtering equipment (AJA international, Inc.). For the thickness measurement of the cermet layer the materials are simultaneously deposited on Si wafers partly covered by a mask. Prior to the deposition process, the chamber is evacuated to lower than $4x10^{-7}$ Torr. The deposition targets are high purity nickel (99.999%, 2" Dia.), tungsten (99.95%, 3" Dia.), Al_2O_3 (99.98%, 2" Dia.), and SiO_2 (99.995%, 3" Dia.). DC power is supplied to the metal targets (Ni, W) to deposit the metal layer and for the metal particle. The dielectric layer is deposited by RF magnetron sputtering. Co-sputtering is employed to deposit the cermet layers. The metal fill fractions of the cermet layers are controlled by independent input power control to the corresponding targets. The complete deposition process is performed in an argon plasma environment at a pressure of 3 mTorr. The detailed preparation parameters are summarized in table1.

Regarding the thermal stability the fabricated solar absorbers are characterized in terms of their phase, morphology, and optical properties before and after annealing them at 600 ℃ for 7 days at a vacuum pressure of ~$5x10^{-3}$ Torr using a tubular furnace. The X-ray diffraction (XRD) patterns are obtained using a PANalytical multipurpose diffractometer with an X'Celerator detector and Cu Kα radiation (λ = 1.54056 Å) operating at 45 kV and 40 mA. Raman scattering spectra measurements are carried out on a T64000 Raman system (Horiba Jobin Yvon) at room temperature. The excitation source is the 514 nm laser line of an air cooled Ar-ion laser. The thickness of the cermet films are measured with an Alpha-step 200 Profilometer (Tencor). The growth rates of metal and dielectric layers are measured by a quartz crystal monitor equipped in the sputterring system. The morphology and roughness of the films are measured with a Veeco Dimensions 3000 Atomic Force Microscope (AFM). The spectral bidirectional reflectance are measured at room temperature with a Spectrophotometer by Varian (Cary 500i, angle of incidence 8 º, absolute spectral reflectance

accessory) covering the wavelength range of 0.3 – 1.8 μm, and with an FT-IR Spectrometer by Thermo Scientific (Nicolet 6700, angle of incidence 12 °) covering the wavelength range of 1.8 – 20 μm. The latter (relative measurement) requires a reference with known spectral reflectance which is chosen to be a specular gold mirror (Thorlabs). The indirectly obtained emittance values of solar absorbers from spectral reflectance data measured close to room temperature significantly underestimates the emittance at elevated temperature because it ignores the temperature dependence of the dielectric constants.[2, 16] For that reason, the solar absorptance and total hemispherical emittance of a fabricated solar absorber (S-W/SS) with thermally stable and most promising spectral reflectance data is directly measured at elevated temperatures (up to 500 °C) using simple steady state calorimetric methods.[16] The sample is attached to a heater assembly and suspended in a vacuum chamber. The electrical heater power input is directly related to the radiation heat loss from the sample surface. Thus, the total hemispherical emittance can be calculated with the electrical heater power inputs and the measured sample and surrounding temperatures. The solar absorptance is measured at elevated temperatures using a solar simulator. The sample/heater assembly is suspended in the vacuum chamber facing a viewport allowing the solar simulator beam to irradiate the sample surface. The solar absorptance can be obtained by varying the incident radiation power onto the sample and measuring the corresponding electric heater power adjustments to maintain the sample surface at a constant temperature.

Author contributions

F. C. conceived the film configuration, implemented the experimental studies, analyzed the results and prepared manuscript. D. K. characterized spectral properties of solar absorber, measured solar absorptance and total hemispherical emittance, analyzed the results and prepared manuscript. T. S.

analyzed the results. Y. L. measured Raman spectra. G. C. directed research at MIT. Z. F. R. directed research at UH. F. C. and D. K. contributed equally to this work.

Acknowledgments

The authors would like to thank Dr. Jeffrey Chou and Tim McClure for discussions on spectral reflectance experiments and Dr. Alexander Litvinchuk at TcSUH for the measurement of Raman spectra. This work was partially supported by "Concentrated Solar Thermoelectric Power (CSP)", a DOE SunShot CSP grant, under award number DE-EE0005806 and "Solid State Solar-Thermal Energy Conversion Center (S^3TEC)", an Energy Frontier Research Center funded by the U.S. Department of Energy, Office of Science, Office of Basic Energy Science under award number DE-SC0001299/DE-FG02-09ER46577 (GC and ZFR).

Received: ((will be filled in by the editorial staff))
Revised: ((will be filled in by the editorial staff))
Published online: ((will be filled in by the editorial staff))

[1] a) F. Mauthner, W. Weiss, in *Markets and Contribution to the Energy Supply 2011*, Solar Heating & Cooling Programme International Energy Agency, **2013**; b) D. Kraemer, B. Poudel, H. P. Feng, J. C. Caylor, B. Yu, X. Yan, Y. Ma, X. W. Wang, D. Z. Wang, A. Muto, K. McEnaney, M. Chiesa, Z. F. Ren, G. Chen, *Nat Mater* **2011**, 10, 532; c) D. Mills, *Sol Energy* **2004**, 76, 19; d) A. Lenert, D. M. Bierman, Y. Nam, W. R. Chan, I. Celanovic, M. Soljacic, E. N. Wang, *Nat Nanotechnol* **2014**, 9, 126; e) K. McEnaney, D. Kraemer, G. Chen, in *Annual Review of Heat Transfer*, Vol. 15 (Eds: G. Chen, V. Pradad, Y. Jaluria, J. Karni), Begell House, Redding, CT **2012**, 179.

[2] C. E. Kennedy, National Renewable Energy Laboratory, **2002**.

[3] K. McEnaney, in *Department of Mechanical Engineering*, Master, Massachusetts Institute of Technology, Cambridge **2010**.

[4] F. Cao, K. McEnaney, G. Chen, Z. Ren, *Energ Environ Sci* **2014**, 7, 1615.

[5] a) H. C. Barshilia, P. Kumar, K. S. Rajam, A. Biswas, *Sol Energ Mat Sol C*, Vol. 95, **2011**, 1707; b) Z. Li, J. Zhao, L. Ren, *Sol Energ Mat Sol C* **2012**, 105, 90.

[6] a) Q.-C. Zhang, *Sol Energ Mat Sol C* **1998**, 52, 95; K. Rajanna, S. Srinivasulu, M. M. Nayak, S. Mohan, *J Mater Sci Lett* **1993**, 12, 37; b) F. Garnich, E. Sailer, *Sol Energ Mater* **1990**, 20, 81; J. A. Wang, B. C. Wei, Q. R. Wei, D. J. Li, *Phys Status Solidi A* **2011**, 208, 664; c) Q.-C. Zhang, Y. G. Shen, *Sol Energ Mat Sol C* **2004**, 81, 25; d) Q.-C. Zhang, *J Phys D Appl Phys* **2001**, 34, 3113; e) Q.-C. Zhang, *J Phys D Appl Phys* **1998**, 31, 355; f) M. Farooq, A. A. Green, M. G. Hutchins, Sol Energ Mat Sol C **1998**, 54, 67; g) Q.-C. Zhang, *Journal of Vacuum Science & Technology A: Vacuum, Surfaces, and Films* **1997**, 15, 2842.

[7] J. Cheng, C. Wang, W. Wang, X. Du, Y. Liu, Y. Xue, T. Wang, B. Chen, *Sol Energ Mat Sol C* **2013**, 109, 204.

[8] A. Antonaia, A. Castaldo, M. L. Addonizio, S. Esposito, *Sol Energ Mat Sol C* **2010**, 94, 1604.

[9] D. Xinkang, W. Cong, W. Tianmin, Z. Long, C. Buliang, R. Ning, *Thin Solid Films* **2008**, 516, 3971.

[10] a) Y. Xue, C. Wang, W. Wang, Y. Liu, Y. Wu, Y. Ning, Y. Sun, *Sol Energy* **2013**, 96, 113; b) S. N. Kumar, L. K. Malhotra, K. L. Chopra, *Sol Energ Mater* **1983**, 7, 439.

[11] S. Esposito, A. Antonaia, M. L. Addonizio, S. Aprea, *Thin Solid Films* **2009**, 517, 6000.

[12] B. A. Moys, *Thin Solid Films* **1974**, 21, 145.

[13] a) Y. Liu, C. Wang, Y. F. Xue, Sol Energ Mat Sol C **2012**, 96, 131; b) Q.-C. Zhang, D. R. Mills, *J Appl Phys* **1992**, 72, 3013.

[14] J. Ruiz-Fuertes, D. Errandonea, S. López-Moreno, J. González, O. Gomis, R. Vilaplana, F. J. Manjón, A. Muñoz, P. Rodríguez-Hernández, A. Friedrich, I. A. Tupitsyna, L. L. Nagornaya, *Phys Rev B* **2011**, 83, 214112.

[15] Z. Q. Chen, F. Wang, P. Huang, T. J. Lu, K. W. Xu, *J Nanomater* **2013** 2013, 252965.

[16] D. Kraemer, K. McEnaney, F. Cao, Z. F. Ren, G. Chen, *Submited to Sol Energ Mat Sol* **2014**.

[17] A. Sakurai, H.Tanikawa, M. Yamada, presented at 7th Inter. Sym. on Rad. Trans, A wide-angle cermet-based solar selective absorber for high temperature applications, Kusadasi, June, **2013**.

The table of contents

The iron diffusion from stainless steel substrate is suppressed by introducing a thick tungsten layer between substrate and absorber coatings. The spectrally-selective solar absorber with tungsten layer demonstrates a long-term thermal stability at 600 ^{o}C, a stable solar absorptance of ~0.90 and total hemispherical emittance of 0.15 at 500 ℃.

Keyword solar absorber, cermet, solar absorptance, thermal emittance, spectral selectivity.

Feng Cao, Daniel Kraemer, Tianyi Sun, Yucheng Lan, Gang Chen,* and Zhifeng Ren*

Title Enhanced Thermal Stability of W-Ni-Al_2O_3 Cermet-based Spectrally Selective Solar Absorbers with W Infrared Reflector

ToC figure